

## Cyclic amino acid linkers stabilizing key loops of brain derived neurotrophic factor

José Luis Baeza<sup>a</sup>, Beatriz G. de la Torre<sup>b</sup>, Clara M. Santiveri<sup>c</sup>, Ramiro D. Almeida<sup>d</sup>,  
M. Teresa García-López<sup>a</sup>, Guillermo Gerona-Navarro<sup>d</sup>, Samie R. Jaffrey<sup>d</sup>, M. Ángeles Jiménez<sup>c</sup>,  
David Andreu<sup>b</sup>, Rosario González-Muñiz<sup>a</sup>, Mercedes Martín-Martínez<sup>a,\*</sup>

<sup>a</sup> Instituto de Química Médica (IQM-CSIC), Juan de la Cierva 3, Madrid 28006, Spain

<sup>b</sup> Dpto. de Ciencias Experimentales y de la Salud, Universidad Pompeu Fabra, Parc de Recerca Biomèdica de Barcelona, Dr. Aiguader 88, Barcelona 08003, Spain

<sup>c</sup> Instituto de Química Física Rocasolano (IQFR-CSIC), Serrano 119, Madrid 28006, Spain

<sup>d</sup> Dept. of Pharmacology, Weill Medical College of Cornell University, 1300 York Avenue, Box 70, Whitney Pavilion, W-506, New York, NY 10021, USA

### ARTICLE INFO

#### Article history:

Received 12 August 2011

Revised 28 October 2011

Accepted 30 October 2011

Available online 6 November 2011

#### Keywords:

BDNF

Growth factors

Peptides

Secondary peptide structure mimetics

$\beta$ -Turn

### ABSTRACT

Based on  $\beta$ -turn-like BDNF loops 2 and 4, involved in receptor interaction, cyclic peptide replicas were designed, synthesized and tested. In addition to the native turn residues, the cyclic peptides include a linker unit between the *N*- and *C*-termini, selected by molecular modeling among various non-proteinogenic cyclic amino acids. NMR conformational studies showed that most of the cyclic peptides were able to adopt turn-like structures. Several of the analogues displayed significant inhibition of the BDNF-induced TrkB receptor phosphorylation, and hence could be useful templates for developing improved antagonists for this receptor.

© 2011 Elsevier Ltd. All rights reserved.

Brain-derived neurotrophic factor (BDNF) is a member of the neurotrophin (NT) family, which includes dimeric factors essential in the development and maintenance of both central and peripheral nervous systems, and is also involved in other disorders such as obesity and cancer.<sup>1–4</sup> The biological functions of BDNF are mediated through its interaction with two transmembrane receptors, the tyrosine kinase receptor TrkB, to which it binds selectively, and a non-tyrosine kinase, p75.<sup>5,6</sup> The therapeutic potential of NTs is limited by short *in vivo* lifetimes, unsatisfactory pharmacokinetics and unfavorable side effects.<sup>3,7,8</sup> One approach to overcome these drawbacks would be the development of small NT mimetics with better properties.

X-ray and mutagenesis studies have allowed the identification of several NT loops essential for the interaction with their receptors. In particular, BDNF binding to TrkB involves loops 2 (Val<sup>44</sup>-Ser-Lys-Gly<sup>47</sup>) and 4 (Asp<sup>93</sup>-Ser-Lys-Lys-Arg<sup>97</sup>), with  $\beta$ -turn-like structures centered at Ser<sup>45</sup>-Leu<sup>46</sup> and Ser<sup>94</sup>-Lys<sup>95</sup>, respectively.<sup>6,9–14</sup>  $\beta$ -Turns are non-repetitive secondary structure elements formed by four residues, in which the distance between the first and fourth  $\alpha$ -carbon is less than 7 Å, often stabilized by

a hydrogen bond between the CO group of the first residue and the NH of the fourth.<sup>15,16</sup>

An approach to the search for  $\beta$ -turn mimetics is the preparation of cyclic peptides containing the amino acid sequence of the turn. Thus, several cyclic analogues of key BDNF loops, quite frequently cyclized by disulfide-bridges, were able to promote or inhibit BDNF-mediated neuronal survival.<sup>11–14</sup>

To develop new constrained cyclic analogues of BDNF loops 2 and 4, we focused on small, rigid, non-proteinogenic amino acid linkers connecting the *N*- and *C*-termini of these loops. These linkers should favor the adoption of a native-like  $\beta$ -turn conformation, while their cyclic nature could enhance peptide stability by decreasing proteolytic degradation. To the first end, we explored bifunctional compounds such as 2-, 3- and 4-aminobenzoic- or 2-, 3- and 4-aminohexanoic acids, as well as 2-alkyl-2-carboxyazetidines derivatives previously reported by our group.<sup>17,18</sup> A molecular dynamics (MD) conformational search of cyclic peptides incorporating these linkers in all possible stereochemistries suggested (1*S*,2*S*)-2-aminocyclohexanoic acid (BAC<sub>6</sub>C), (*S*)-2-carboxylate-azetidines (Azg),<sup>19</sup> (*S*)- and (*R*)-2-carboxylate-2-methylazetidines [(*S*) and (*R*)-Aza] as the most appropriate for loop 2, and BAC<sub>6</sub>C and Azg for loop 4.

A detailed comparison between the minimum energy conformers of loop 2 mimetics cyclo(Val-Ser-Lys-Gly-Xaa) and the BDNF

\* Corresponding author.

E-mail address: [mercedes@iqm.csic.es](mailto:mercedes@iqm.csic.es) (M. Martín-Martínez).

native loop showed that the larger deviations are around Val<sup>44</sup> residue (Fig. 1A). A better fit at position 44 was obtained by replacing Gly<sup>47</sup> by  $\beta$ -Ala, but this in turn caused a divergence at the  $i + 3$  position of the  $\beta$ -turn ( $\beta$ -Ala) (Fig. 1B). With the aim of finding the appropriate spatial disposition of key groups, peptides incorporating each of the above mentioned linkers, with either Gly or  $\beta$ -Ala at the  $i + 3$  position, were selected for study (derivatives **1–6**, Fig. 2).

For cyclic loop 4 mimetics, both BAc<sub>6</sub>c or Azg linkers led to minimum energy conformers with 3D structures very similar to the native loop at the turn region (Fig. 1C). Accordingly, compounds **7**, cyclo[Asp-Ser-Lys-Lys-Arg-BAc<sub>6</sub>c], and **8**, cyclo[Asp-Ser-Lys-Lys-Arg-Azg], were selected for study.

The BDNF mimetics were prepared by solid-phase methods on a Wang resin, using Fmoc/<sup>t</sup>Bu chemistry for chain elongation, followed by intramolecular on-resin cyclization. Fmoc-Lys-OAl<sup>20</sup> was coupled through its side chain to the resin yielding **9**, to which the corresponding Fmoc-protected amino acids were sequentially incorporated into the desired **10–15** sequences (Scheme 1). Intramolecular cyclization of the resin-bound linear peptides required prior removal of the allyl group, followed by deprotection of the *N*-terminal Fmoc and amide bond formation (Scheme 1, route A). Subsequent cleavage and deprotection of the resin-bound cyclic peptides led to end-products **1–6**.<sup>21</sup> HPLC analysis of the crude products showed the presence of a minor peak assigned to the cyclic decapeptides **16–21** (dimers),<sup>22</sup> and of even smaller amounts of the 15-residue trimer. Dimer formation was interpreted as the result of concomitant inter-chain acylation between the *N*-terminal amino group of one linear sequence and the Lys backbone carboxyl of the neighboring sequence (Scheme 1, route B).

Preparative HPLC purification of the **1–6** synthetic crudes allowed isolation of the [(*R,S*)-**6**] but not the [(*R,S*)-**5**] pair of diastereoisomers. On the other hand, while **3** and **4** were obtained in high purity, they were unstable upon storage, yielding linear Azg-Val-Ser-Lys-Xaa [Xaa = Gly (**22**) or  $\beta$ Ala (**23**)], as a result of Yaa-Azg amide bond cleavage.

The synthesis of loop 4 mimetics **7** and **8** (Scheme 2) followed a similar strategy to that of loop 2 analogues. Cyclic hexapeptide **7** was obtained in 11% yield, together with a 7% of cyclic dimer **24**, while the Azg-containing analogue **8** could only be obtained in a 1% yield.<sup>23</sup>

Compounds **1–8** and dimers **17**, **20a** and **24** were examined by NMR. Spectral analysis of **3–6** was complex due to the *cis/trans* equilibrium presented by Aza and Azg. Derivative (*R*)-**6** was only partially assigned because of its incomplete separation from one of the dimers.

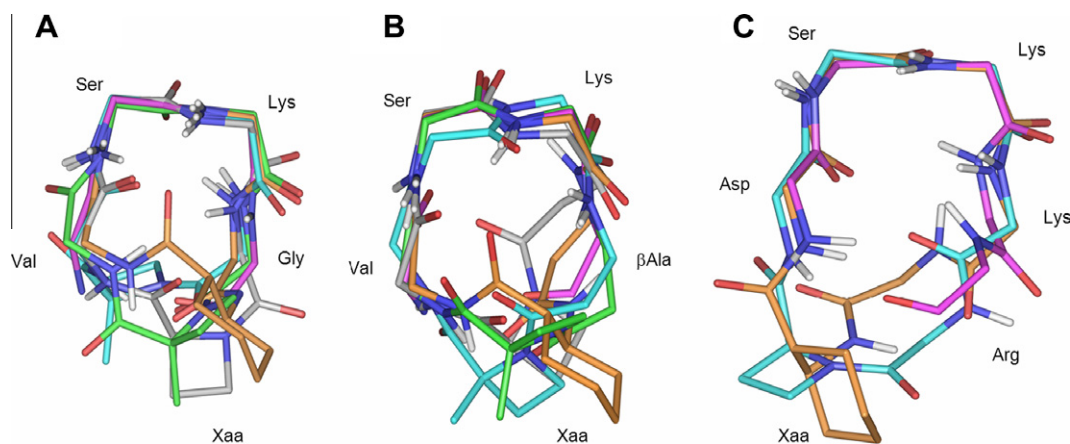
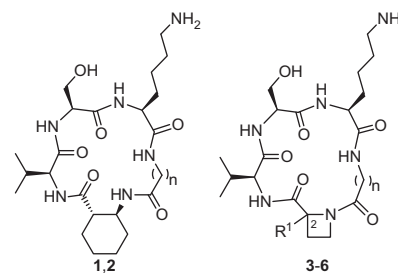


**Figure 1.** (A) Backbone atoms of the global energy minimum conformers of cyclo(Val-Ser-Lys-Gly-Xaa) superimposed on native BDNF loop 2 (C atoms in pink, pdb code 1bnd). (B) Same as A for cyclo(Val-Ser-Lys- $\beta$ Ala-Xaa). (C) Backbone atoms of the global minimum conformers of cyclo(Asp-Ser-Lys-Lys-Arg-Xaa) superimposed on native BDNF loop 4 (C atoms in pink, pdb code 1bnd). Xaa = BAc<sub>6</sub>c (A, B and C: orange), Azg (A and B: grey, C: cyan), (*S*)-Aza (A and B: green), (*R*)-Aza (A and B: cyan).



Comp.	1	2	3	4	( <i>R</i> )-5	( <i>S</i> )-5	( <i>R</i> )-6	( <i>S</i> )-6
N	1	2	1	2	1			2
R <sup>1</sup>				H			Me	
linker	BAc <sub>6</sub> c		Azg		Aza			

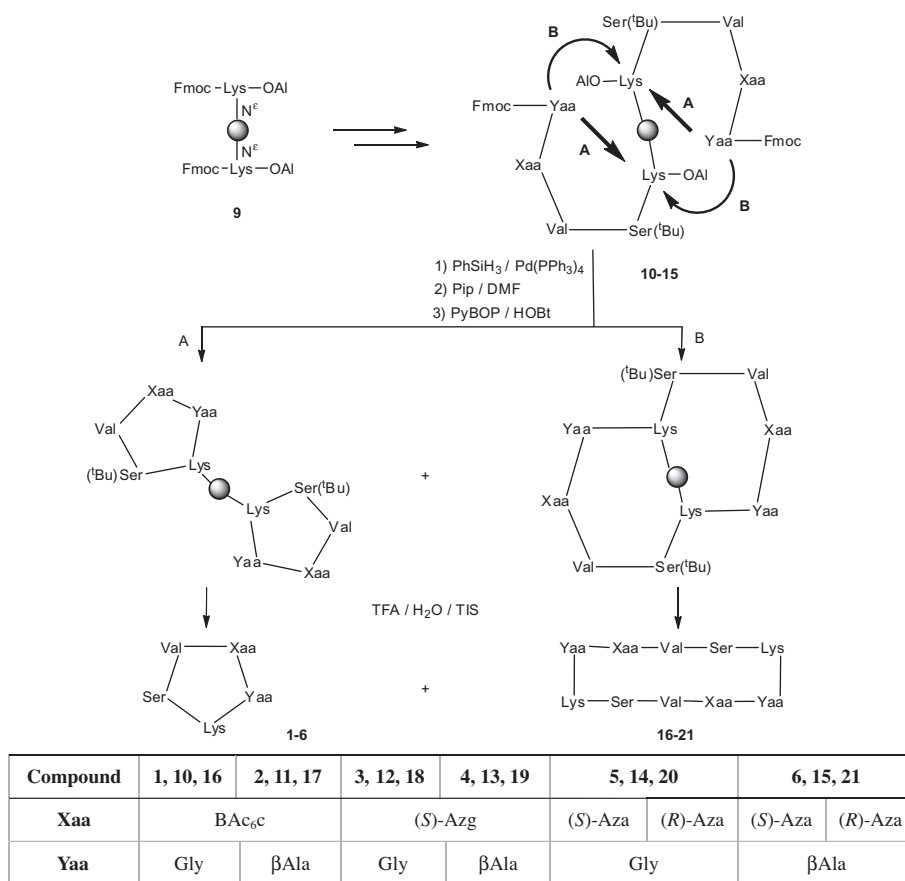
**Figure 2.** Cyclic peptides **1–6**, designed as mimetics of BDNF loop 2.

*Trans* and *cis* rotamers were differentiated on the basis of characteristic NOEs of the Yaa residue H <sub>$\alpha$</sub>  proton (Gly or  $\beta$ -Ala) either with azetidine H-4 proton for the *trans*-isomers or with H-2 or methyl protons for the *cis*. The assignment was confirmed by the anisotropy criterion.<sup>24</sup> For cyclo(Val-Ser-Lys-Yaa-Azg) (**3** and **4**), the *cis*-isomers were the major species, whereas for Aza-bearing (*R*)-**5**/*S*-**5** and (*S*)-**6** analogues the *trans*-isomers predominated (Table ST1). As expected, the *trans* percentage increased if the C-2 of the azetidine ring was disubstituted.<sup>17,18</sup>

The absolute stereochemistry of the Aza carbon C-2 in each diastereoisomer of the (*R,S*)-**5** mixture, and in the non-contaminated diastereoisomer of compound **6**, was assigned on the basis of NOEs and detailed chemical shift comparison with (*S*)-Azg derivatives **3** and **4**.

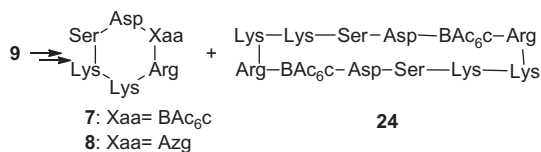
Chemical shift analysis indicated that the cyclic derivatives have non-random conformations, as expected from MD simulations. In particular, the H <sub>$\alpha$</sub> , C <sub>$\alpha$</sub>  and C $\beta$  chemical shifts of proteinogenic amino acids in the cyclic analogues deviated strongly from random coil values in most of the species (>0.1 and >1 ppm, for <sup>1</sup>H and <sup>13</sup>C  $\delta$ -values, respectively; Figures 3 and SF1), indicating that compounds **1–7** adopt some ordered conformations.

Loop 2 cyclic peptides, in general, showed similar patterns of  $\Delta\delta$ -values, that is negative values for the H <sub>$\alpha$</sub>  proton and C $\beta$  carbon, and positive for the C <sub>$\alpha$</sub>  carbon (Figures 3 and SF1), which indicate that Val, Ser and Lys residues adopt  $\psi$  angles in the right-handed  $\alpha$  region of the Ramachandran map ( $\alpha_R$ ),<sup>25–27</sup> as observed for Ser<sup>45</sup>



BAC<sub>6</sub>c = (1S,2S)-2-aminocyclohexanoic acid, Azg = azetidine-2-carboxylate, Aza = 2-methylazetidine-2-carboxylate.

Scheme 1. Synthesis of BDNF loop 2 mimetics.



Scheme 2. Synthesis of BDNF loop 4 mimetics.

and Lys<sup>46</sup> in the native IV β-turn (BDNF/NT3 complex, pdb code 1bnd),<sup>9</sup> but not for Val<sup>44</sup> that is in the β region.

The  $\Delta\delta$  values of loop 4 analogue **7** are suggestive of Ser<sup>94</sup>, Lys<sup>95</sup>, and Arg<sup>97</sup> being in the  $\alpha_R$  region of the Ramachandran map. This is compatible with the  $i + 1$  and  $i + 2$  positions occupied by Ser<sup>94</sup> and Lys<sup>95</sup> in the native loop 4 conformation. Thus, the BAC<sub>6</sub>c linker is also able to stabilize the central residues of loop 4 in a turn-like conformation.

Next, we analyzed the temperature dependence of the amide protons ( $\Delta\delta/\Delta T$ ). By commonly accepted criteria,<sup>24,28,29</sup> at least one NH amide proton is solvent-protected in the 5-residue cyclic loop 2 derivatives ( $\Delta\delta/\Delta T < 4$  ppb K<sup>-1</sup>, Table 1), except for compound **1** and the *trans* rotamers of **4** and (S)-**6**, for which the smaller temperature coefficients are in the uncertainty range (4–5 ppb K<sup>-1</sup>). Interestingly, at least in one of the rotamers, the solvent-shielded NH amide protons include either Val<sup>44</sup> or Xaa<sup>47</sup>, whose amide protons are hydrogen-bonded in the native BDNF loop 2. It is worth noting that, in the MD studies, the NH amide of Val<sup>44</sup> is hydrogen-bonded to the CO of Xaa<sup>47</sup>, a characteristic of the azetidine-induced  $\gamma$ -turn.<sup>17,18</sup> Replacement of Gly for  $\beta$ -Ala increased the number of conformers with a hydrogen

bond-stabilized  $\beta$ -turn (NH proton of the Xaa residue involved). On the whole, the BAC<sub>6</sub>c linker stabilizes better Ser ( $i + 1$   $\beta$ -turn-residue), while Azg and Aza are suitable for Lys ( $i + 2$   $\beta$ -turn residue).

The conformational behavior of cyclic decapeptides **17** and **20a** differed from their 5-residue counterparts. Both peptides showed  $\Delta\delta$  profiles for Val<sup>44</sup>, Ser<sup>45</sup> and Lys<sup>46</sup> characteristic of  $\beta$ -strands, with positive  $\Delta\delta_{H\alpha}$  and  $\Delta\delta_{C\beta}$  and negative  $\Delta\delta_{C\alpha}$  values (Figures 3 and SF1). Only the Val<sup>44</sup> NH proton of peptide **20a** was solvent-shielded (Table 1), and a non-sequential NOE cross-peak between the methyl groups of Val<sup>44</sup> and the H $\alpha$  proton of Lys<sup>46</sup> was observed. These data indicate that peptides **17** and **20a** might adopt antiparallel  $\beta$ -sheets. The different ability to fit a turn conformation of sequences containing  $\beta$ Ala-BAC<sub>6</sub>c (**17**) and Gly-Aza (**20a**) correlates with the well-known tendency of azetidine to induce turns,<sup>17,18</sup> and might account for the higher flexibility of the antiparallel  $\beta$ -sheet formed by peptide **17**.

In the loop 4 analogue **7**, the amide temperature coefficients suggested that the NH amide protons of Ser<sup>94</sup> (–3.0 ppb K<sup>-1</sup>) and Arg<sup>97</sup> (–3.5 ppb K<sup>-1</sup>) were involved in intramolecular hydrogen bonds. Both amide protons were found to participate in hydrogen bonds in the molecular modeling studies, NH-Ser<sup>94</sup>...CO-Arg<sup>97</sup>/BAC<sub>6</sub>c and the NH-Arg<sup>97</sup>...CO-Ser<sup>94</sup>. In contrast, the amide proton of Lys<sup>96</sup> (–2.5 ppb K<sup>-1</sup>) is the only one involved in an intramolecular hydrogen bond in cyclic dodecapeptide **24**. This indicates a different overall structure for compounds **24** and **7**, though Ser<sup>94</sup> and Lys<sup>95</sup> maintain a kind of native-like turn in both.

Finally, the capacity of BDNF loop 2 and 4 mimetics, **1–7** and their dimeric counterparts **16–20** and **24**, to either induce or inhibit TrkB phosphorylation was evaluated in hippocampal neuron

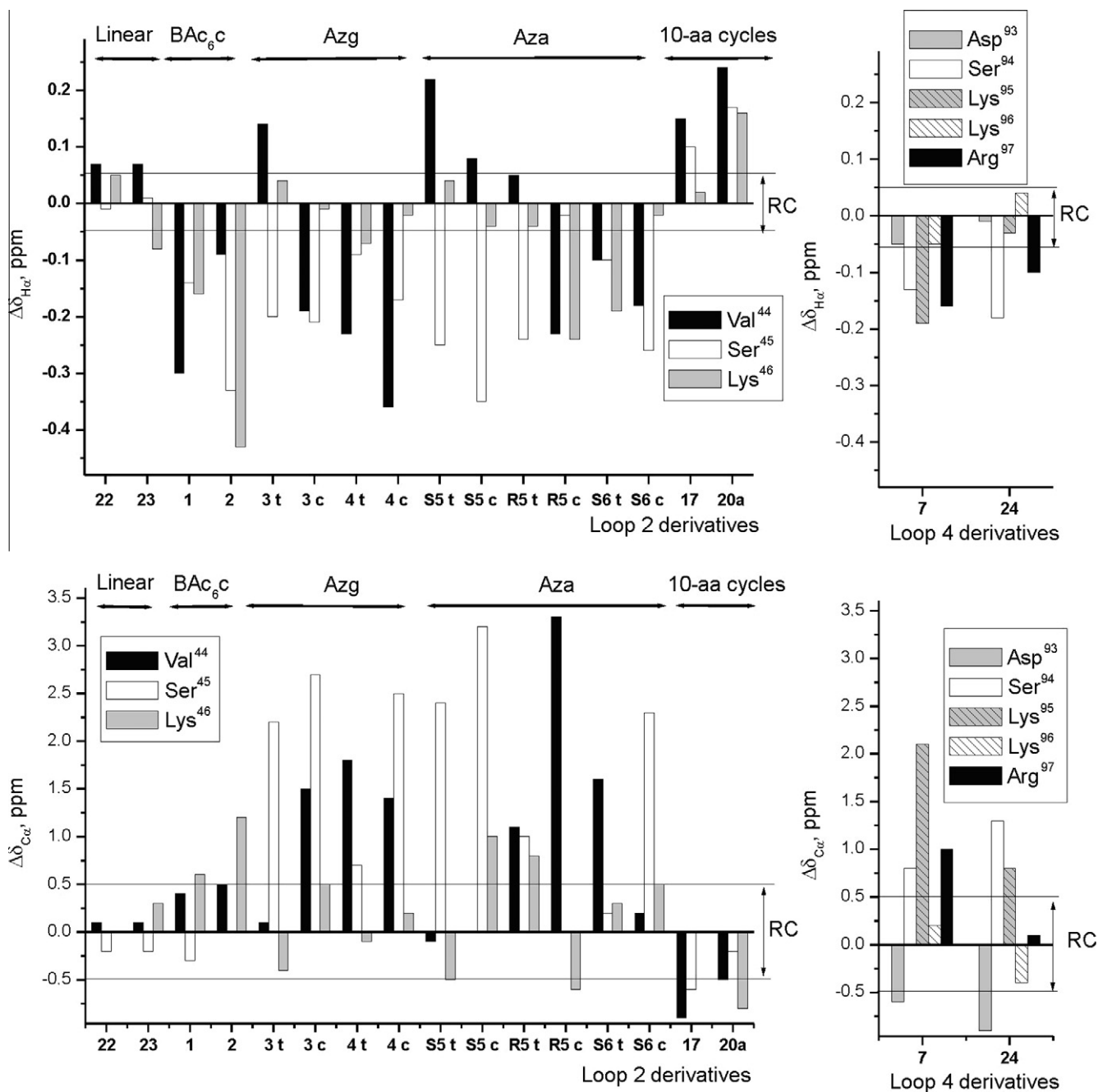


**Figure 3.** Histograms showing the  $\Delta\delta_{H\alpha}$  and  $\Delta\delta_{C\alpha}$  profiles ( $\Delta\delta = \delta^{\text{observed}} - \delta^{\text{random coil}}$ , ppm) for natural amino acids in loop 2 and loop 4 derivatives. *Trans* and *cis* rotamers are indicated by *t* and *c*. The random coil range is indicated by two horizontal lines.

cultures. Assays in the absence of BDNF indicated that these peptides were not able to induce TrkB autophosphorylation, hence they do not behave as agonists. Experiments aimed to evaluate their inhibitory capacity showed that, in general, the smaller cyclic peptides are inactive, with the exception of loop 4 mimetic **7** [cyclo(Asp-Ser-Lys-Lys-Arg-BAC<sub>6</sub>c)], which was able to significantly inhibit BDNF-induced phosphorylation, as shown by the decreased intensity of the phosphorylated TrkB band in Figure 4. Additionally, several of the dimers, in particular **20b** and **24**, also inhibited the BDNF-induced phosphorylation. The fact that loop 2 dimer **20b** proved to be active, whereas the corresponding pentapeptide (R,S)-**5** was not, might be due to the different structure adopted by the former. Alternatively, the higher conformational flexibility

of **20b** might allow it to adopt a 3D arrangement suitable for binding to the receptor by an induced-fit mechanism.

On the whole, NMR conformational analyses suggested that BAC<sub>6</sub>c, Aza and Azg are suitable linkers for stabilizing the central residues of BDNF loops into a  $\beta$ -turn-like conformation. The azetidine-based linkers are best suited to reproduce the native conformation at the *i* + 1 residue, while BAC<sub>6</sub>c is preferred for the *i* + 2. NMR data for loop 2 and 4 dimers show them adopting  $\beta$ -sheet-like structures with the non-proteogenic linkers located, as expected, at the turn, in particular the azetidines. Biological data are promising for **7**, **20b** and **24**. For **7** in particular, the ability to inhibit TrkB phosphorylation, as well as the substantial size reduction compared to BDNF, can be considered a good starting point for the

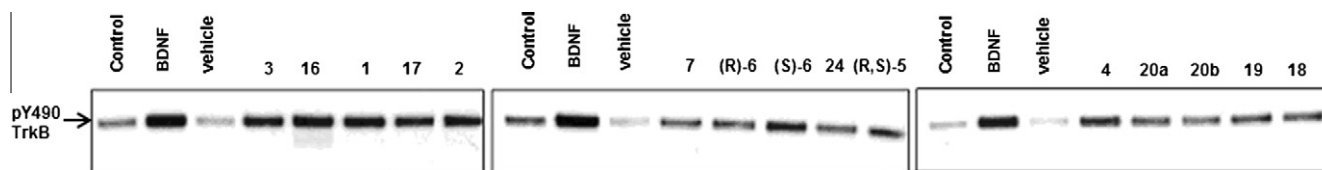


**Figure 4.** Western Blot analysis of the inhibition of the TrkB phosphorylation induced by BDNF. For the assays after a pre-incubation with 100  $\mu\text{M}$  of each compound, BDNF (10 ng/ml) was added. The band corresponding to phosphorylated TrkB at Tyr490 is shown.

**Table 1**

Temperature coefficients of the NH protons ( $\Delta\delta/\Delta T$ , ppb  $\text{K}^{-1}$ ) for BDNF loop 2 mimetics<sup>a</sup>

Compound	Iso. <sup>b</sup>	NH $\Delta\delta/\Delta T$ (ppb $\text{K}^{-1}$ )			
		Val <sup>44</sup>	Ser <sup>45</sup>	Lys <sup>46</sup>	Xaa <sup>47</sup>
c[VSKG-BAC <sub>6</sub> C]	<b>1</b>	-7.5	-5.5	-6.5	-5.0
c[VSK- $\beta$ A-BAC <sub>6</sub> C]	<b>2</b>	-6.5	-8.5	-7.5	<b>-2.5</b>
c[VSKG-(S)-Azg]	<b>3</b>	-7.0	-5.5	<b>-3.0</b>	-8.0
c[VSK- $\beta$ A-(S)-Azg]	<i>c</i>	<b>-4.0</b>	-5.5	<b>-2.0</b>	-8.5
	<i>t</i>	-10.0	-6.5	<b>-0.5</b>	<b>-1.0</b>
c[VSKG-(S)-Aza]	<i>c</i>	-7.5	-4.5	-5.0	-5.0
	(S)- <b>5</b>	-7.0	<b>-3.5</b>	<b>-2.0</b>	-10.0
c[VSKG-(R)-Aza]	<i>c</i>	-4.5	-5.0	<b>-2.0</b>	-8.5
	(R)- <b>5</b>	-5.5	-7.0	-8.0	<b>-2.0</b>
c[VSK- $\beta$ A-(S)-Aza]	<i>c</i>	<b>-1.0</b>	-8.5	<b>-4.0</b>	-5.0
	(S)- <b>6</b>	-8.0	-7.0	<b>-2.5</b>	<b>-2.0</b>
c[VSK- $\beta$ A-BAC <sub>6</sub> C] <sub>2</sub>	<i>c</i>	-7.5	-4.5	-7.0	-5.0
	<b>17</b>	-9.0	-5.5	-8.0	-7.5
c[VSKG-Aza] <sub>2</sub>	<b>20a</b>	<i>t-t</i>	<b>0.0</b>	-9.0	-6.5

<sup>a</sup> Absolute values equal to or less than 4.0 ppb  $\text{K}^{-1}$  in bold. One letter code for proteinogenic amino acids: V: Val, S: Ser, K: Lys, Xaa: Gly or  $\beta$ -Ala.  $\Delta\delta/\Delta T$  of BAC<sub>6</sub>C NH is always below -6 ppb  $\text{K}^{-1}$ .

<sup>b</sup> *c*: cis, *t*: trans.

future development of TrkB receptor antagonists with improved activity profiles.

## Acknowledgments

This work was supported by the Spanish Ministry of Education and Science (SAF 2009-09323 & CTQ2008-00080/BQU). J.L.B. was a predoctoral FPI fellow.

## Supplementary data

Supplementary data (synthetic procedures, molecular modeling, biological evaluation and NMR parameters for all compounds) associated with this article can be found, in the online version, at doi:10.1016/j.bmcl.2011.10.107.

## References and notes

- Chao, M. V. *Nat. Rev. Neurosci.* **2003**, *4*, 299.
- Bibel, M.; Barde, Y.-A. *Genes Dev.* **2000**, *14*, 2919.
- Nagahara, A. H.; Tuszynski, M. H. *Nat. Rev. Drug Disc.* **2011**, *10*, 209.
- Nakagawara, A. *Cancer Lett.* **2001**, *169*, 107.
- Pattarawarapan, M.; Burgess, K. J. *Med. Chem.* **2003**, *46*, 5277.
- Longo, F. M.; Xie, Y.; Massa, M. *Curr. Med. Chem.—Central Nervous System Agents* **2005**, *5*, 29.
- Saragovi, H. U.; Burgess, K. *Exp. Opin. Ther. Patents* **1999**, *9*, 737.
- Apfel, S. C. *Int. Rev. Neurobiol.* **2002**, *50*, 393.
- Robinson, R. C.; Radziejewski, C.; Stuart, D. I.; Jones, E. Y. *Biochemistry* **1995**, *34*, 4138.

- Robinson, R. C.; Radziejewski, C.; Spraggon, G.; Greenwald, J.; Kostura, M. R.; Burtnick, L. D.; Stuart, D. I.; Choe, S.; Jones, E. Y. *Protein Sci.* **1999**, *8*, 2589.
- O'Leary, P. D.; Hughes, R. A. J. *Neurochem.* **1998**, *70*, 1712.
- Fletcher, J. M.; Hughes, R. A. J. *Pept. Sci.* **2006**, *12*, 515.
- O'Leary, P. D.; Hughes, R. A. J. *Biol. Chem.* **2003**, *278*, 25738.
- Fletcher, J. M.; Morton, C. J.; Zwar, R. A.; Murray, S. S.; O'Leary, P.; Hughes, R. A. J. *Biol. Chem.* **2008**, *283*, 33375.
- Rose, G. D.; Gierasch, L. M.; Smith, J. A. *Adv. Protein Chem.* **1985**, *37*, 1.
- Panasik, N., Jr.; Fleming, P. J.; Rose, G. D. *Protein Sci.* **2005**, *14*, 2910.
- Baeza, J. L.; Gerona-Navarro, G.; Pérez de Vega, M. J.; García-López, M. T.; González-Muñiz, R.; Martín-Martínez, M. J. *Org. Chem.* **2008**, *73*, 1704.
- Baeza, J. L.; Gerona-Navarro, G.; Thompson, K.; Pérez de Vega, M. J.; Infantes, L.; García-López, M. T.; González-Muñiz, R.; Martín-Martínez, M. J. *Org. Chem.* **2009**, *73*, 8203.
- For a new nomenclature of azetidine containing amino acids, see: Bonache, M. A.; García-Martínez, C.; García de Diego, L.; Carreño, C.; Pérez de Vega, M. J.; García-López, M. T.; Ferrer-Montiel, A.; González-Muñiz, R. *ChemMedChem* **2006**, *1*, 429. Azx indicates any azetidine, Azg and Aza refer to Gly and Ala-derived azetidines, respectively.
- Andreu, D.; Ruiz, S.; Carreño, C.; Alsina, J.; Albericio, F.; Jiménez, M. A.; de la Figuera, N.; Herranz, R.; García-López, M. T.; González-Muñiz, R. *J. Am. Chem. Soc.* **1997**, *119*, 10579.
- Cyclo[Val-Ser-Lys-Gly-(1S,2S)-BAC<sub>6</sub>C]-TFA (**1**): Amorphous solid (56% yield, 97% purity). EM (MALDI-TOF): 497.2 [M+1]<sup>+</sup>, 519.1 [M+Na]<sup>+</sup>, 535.1 [M+K]<sup>+</sup>. Cyclo[Val-Ser-Lys- $\beta$ Ala-(1S,2S)-BAC<sub>6</sub>C]-TFA (**2**): Amorphous solid (28% yield, 96% purity). EM (MALDI-TOF): 511.2 [M+1]<sup>+</sup>, 533.1 [M+Na]<sup>+</sup>, 549.1 [M+K]<sup>+</sup>. Cyclo[Val-Ser-Lys-Gly-(S)-Azg]-TFA (**3**): Amorphous solid (17% yield, 95% purity). EM (MALDI-TOF): 455.2 [M+1]<sup>+</sup>, 477.2 [M+Na]<sup>+</sup>, 493.1 [M+K]<sup>+</sup>. Cyclo[Val-Ser-Lys- $\beta$ Ala-(S)-Azg]-TFA (**4**): Amorphous solid (40% yield, 96% purity). EM (MALDI-TOF): 469.3 [M+1]<sup>+</sup>, 491.3 [M+Na]<sup>+</sup>, 507.2 [M+K]<sup>+</sup>. Cyclo[Val-Ser-Lys-Gly-(R,S)-Aza]-TFA [(R,S)-**5**]: Syrup (13% yield). Diastereoisomer ratio R/S: 10:3. Cyclo[Val-Ser-Lys- $\beta$ Ala-(S)-Aza]-TFA [(S)-**6**]: Syrup (6% yield, 97% purity). EM (MALDI-TOF): 483.1 [M+1]<sup>+</sup>, 505.1 [M+Na]<sup>+</sup>, 521.0 [M+K]<sup>+</sup>.
- Cyclo[Val-Ser-Lys-Gly-(1S,2S)-BAC<sub>6</sub>C]<sub>2</sub>-2TFA (**16**): Amorphous solid (6% yield, 90% purity). EM (MALDI-TOF): 993.2 [M+1]<sup>+</sup>, 1015.1 [M+Na]<sup>+</sup>, 1031.1 [M+K]<sup>+</sup>. Cyclo[Val-Ser-Lys- $\beta$ Ala-(1S,2S)-BAC<sub>6</sub>C]<sub>2</sub>-2TFA (**17**): Amorphous solid (4% yield, 85% purity). EM (MALDI-TOF): 1021.4 [M+1]<sup>+</sup>, 1043.3 [M+Na]<sup>+</sup>, 1059.3 [M+K]<sup>+</sup>. Cyclo[Val-Ser-Lys-Gly-Azg]<sub>2</sub>-2TFA (**18**): Amorphous solid (3% yield, 96% purity). EM (MALDI-TOF): 909.2 [M+1]<sup>+</sup>, 931.2 [M+Na]<sup>+</sup>, 947.2 [M+K]<sup>+</sup>. Cyclo[Val-Ser-Lys- $\beta$ Ala-Azg]<sub>2</sub>-2TFA (**19**): Amorphous solid (5% yield, 96% purity). EM (MALDI-TOF): 937.3 [M+1]<sup>+</sup>, 959.3 [M+Na]<sup>+</sup>, 961.3 [M+K]<sup>+</sup>. Cyclo[Val-Ser-Lys-Gly-Aza]<sub>2</sub>-2TFA (**20a**): Syrup (5% yield, 88% purity). EM (MALDI-TOF): 937.3 [M+1]<sup>+</sup>, 959.3 [M+Na]<sup>+</sup>, 975.2 [M+K]<sup>+</sup>. Cyclo[Val-Ser-Lys-Gly-Aza]<sub>2</sub>-2TFA (**20b**): Amorphous solid (4% yield, 89% purity). EM (MALDI-TOF): 937.3 [M+1]<sup>+</sup>, 959.3 [M+Na]<sup>+</sup>, 975.2 [M+K]<sup>+</sup>. Cyclo[Val-Ser-Lys- $\beta$ Ala-Aza]<sub>2</sub>-2TFA (**21**): Syrup (5% yield). EM (MALDI-TOF): 965.1 [M+1]<sup>+</sup>, 987.1 [M+Na]<sup>+</sup>, 1003.1 [M+K]<sup>+</sup>.
- Cyclo[Asp-Ser-Lys-Lys-Arg-(1S,2S)-BAC<sub>6</sub>C]-3TFA (**7**): Amorphous solid (11% yield, 92% purity). EM (MALDI-TOF): 740.4 [M+1]<sup>+</sup>, 762.4 [M+Na]<sup>+</sup>, 778.3 [M+K]<sup>+</sup>. Cyclo[Asp-Ser-Lys-Lys-Arg-(S)-Azg]-3TFA (**8**): Amorphous solid (1% yield, 89% purity). EM (MALDI-TOF): 698.1 [M+1]<sup>+</sup>, 720.0 [M+Na]<sup>+</sup>, 736.1 [M+K]<sup>+</sup>. Cyclo[Asp-Ser-Lys-Lys-Arg-(1S,2S)-BAC<sub>6</sub>C]<sub>2</sub>-6TFA (**24**): Amorphous solid (7% yield, 98% purity). EM (MALDI-TOF): 1479.2 [M+1]<sup>+</sup>, 1501.1 [M+Na]<sup>+</sup>, 1518.1 [M+K]<sup>+</sup>.
- Kessler, H. *Angew. Chem., Int. Ed. Engl.* **1982**, *21*, 512.
- Santiveri, C. M.; Rico, M.; Jiménez, M. A. *J. Biomol. NMR* **2001**, *19*, 331.
- Spera, S.; Bax, A. J. *J. Am. Chem. Soc.* **1991**, *113*, 5490.
- Wishart, D. S.; Sykes, B. D. *Methods Enzymol.* **1994**, *239*, 363.
- Baxter, N. J.; Williamson, M. P. J. *Biolmol. NMR* **1997**, *9*, 359.
- Jiménez, M. A.; Nieto, J. L.; Rico, M.; Santoro, J.; Herranz, J. J. *Mol. Struct.* **1986**, *143*, 435.